Int. J. Heat Mass Transfer. Vol. 34, No. 3, pp. 663–671, 1990
Printed in Great Britain

0017–9310/91 $3.00 + 0.00

Thermocapillary flows of surface melting due to a moving heat flux

J. C. CHEN and Y. C. HUANG
Department of Mechanical Engineering, National Central University, Chung-Li, Taiwan, R.O.C.

(*Received* 11 *September* 1989 *and in final form* 16 *April* 1990)

Abstract—The convective heat transfer and fluid flow that occurs during laser surface melting is examined through a series of numerical computations. The momentum equations and the energy equation are solved by a finite-difference method with a grid-stretching transformation, which places more grid points in the molten region. The effects of thermocapillary convection in the melt and the moving speed of the external heat source on the shape of the solid–liquid interface are considered. Results show that the latent heat of fusion and different dimensionless parameters associated with the moving uniform heat flux have profound effects on determining the melting shape.

1. INTRODUCTION

IN RECENT years, the availability of high power, continuous-wave CO_2 laser beams which provide uniform power intensities over a large cross-sectional area has led to the development of the laser surface melting and alloying technique. This manufacturing technique is of value in producing a surface layer with desired properties such as wear and corrosion resistance. This is why we are concerned with understanding the phenomena of welding pool convection, which affects the size of the molten region and the microstructure of the heat affected zone.

In laser processing a molten portion forms on the surface of the substrate. Kou *et al.* [1] used a heat conduction equation with a finite-difference method to analyse the problem of rapid melting and solidification of a surface subjected to a heat flux with constant moving velocity. But the convection in the melting pool is not taken into consideration. The convection flow pattern in the melt has been experimentally observed by Arata *et al.* [2]. They used a transmission X-ray high-speed cinematography method to reveal the flow motion in cross-sectional Al alloys melted by laser and electron beams. The thermocapillary convection induced by the surface tension gradient along the free surface may be generated due to inhomogeneous heating of the free surface of the molten layer by laser radiation. Usually, thermocapillary convection is coupled with buoyancy-driven convection which is induced by the temperature gradient inside the molten region. Hence, the surface-tension gradient is not the only source of convection motions. The influence of the buoyancy force is minor if the dimensions of the fluid system are small or if the system is exposed to microgravity conditions. The magnitude of maximum melt depths in the laser surface melting and alloying process is in the submicrometer range [3]. Under this condition buoyancy-driven convection is negligible. The large surface-tension gradient is also responsible for the surface deformation along the gas–liquid interface. Because of the rapid resolidification process during laser surface melting, the distortion of the liquid surface is frozen into solid and establishes a roughened ripple surface.

Since the characteristics of the resolidified material may be influenced by the convection-flow pattern during the laser surface melting, it is important to predict the velocity and temperature profile in the melt. The difficulty associated with the surface-melting problem is that there are two kinds of free boundary existing during laser melting. One is the solid–liquid interface and the other is the gas–liquid interface. The position of the free boundaries is unknown and must be determined as a part of the solution. Anthony and Cline [4] considered the one-dimensional fluid flow induced by surface temperature gradient during laser melting and predicted the heights of surface ripple. In their analysis the inertia terms of the Navier–Stokes equations are assumed negligible in the melt. Srinivasan and Basu [5] numerically computed the thermocapillary flow in a rectangular cavity during laser melting. The gas–liquid interface was assumed to be flat with a sinusoidal variation of temperature. Thereafter, Basu and Srinivasan [6] numerically simulated a two-dimensional steady-state laser melting problem but did not consider the moving heat source in the model. Chan *et al.* [7] used a two-dimensional transient model to analyse the convective heat transfer and fluid flow in a laser melted pool. In their model the influences of the latent heat of fusion, the scanning velocity on the cross-section in the direction of the moving heat source, and the deformation of the gas–liquid interface are not considered. Oreper and Szekely [8] represented a transient behaviour of the fluid flow and temperature field in a TIG (tungsten-inert-gas) welding process.

The influence of the thermocapillary convection

NOMENCLATURE

a,b	stretching parameters
B	defined in equation (14)
C_p	specific heat
d	width of the laser beam
g	gravitational acceleration
Gr	Grashof number
H	dimensionless enthalpy
H_l	defined in equation (7d)
H_s	defined in equation (7d)
k	thermal conductivity of liquid and solid
L	dimensionless latent heat of fusion
Ma	Marangoni number
p	dimensionless pressure
Pr	Prandtl number
q	net heat flux
Re	Reynolds number
$S(x,y)$	dimensionless solid–liquid interface
T	dimensionless temperature
T_0	ambient temperature
U	dimensionless scanning velocity of the laser beam
U_c	characteristic velocity in the molten region
u	dimensionless horizontal velocity
v	dimensionless vertical velocity
X	length of the physical domain in the x-direction
x	dimensionless horizontal coordinate
Y	length of the physical domain in the y-direction
y	dimensionless vertical coordinate.

Greek symbols

α	thermal diffusivity
β	volume expansion coefficient
γ	surface-tension temperature coefficient
η, κ	coordinate directions in the computational domain
η_t, κ_t	lengths of the computational domain
μ	dynamic viscosity
ν	kinematic viscosity
ρ	density
σ	surface tension
ξ	vorticity
ϕ	any physical variable
ψ	stream function.

Subscripts

m	melting point
x	derivatives with respect to x
y	derivatives with respect to y.

Superscript

$'$	dimensional value.

coupled with the scanning velocity of a laser beam on the molten region is neglected in the previous literature. The problem examined in the present study is related to that of Kou *et al.* [1]. Consider a laser beam with a constant scanning speed impinging on the surface of a semi-infinite workpiece. In order to simplify the calculation the free surface of the gas–liquid interface is assumed to be flat. The two-dimensional heat- and fluid-flow phenomena during surface melting are analysed using a finite-difference formulation with non-uniform grid transformation. The effect of the latent heat on the melting depth is considered. The influences of Marangoni number, Prandtl number, and scanning speed on the flow fields, the temperature fields, and the melting shape are discussed with physical interpretations.

2. MATHEMATICAL FORMULATION

Consider a rectangular laser beam with a constant scanning speed impinging on the surface of a semi-infinite workpiece. The laser beam has a width d in the scanning direction and length $l \gg d$ in the cross-scanning direction. The system is assumed to be in a quasi-steady state which means that the heat conduction and fluid flow are in a steady state as viewed by an observer located at the centre of the laser beam and travelling with the heat source at the same speed. A schematic diagram of the system is shown in Fig. 1. The origin of the moving coordinates is fixed at the centre of the heat source. The heat conduction and fluid flow are primarily concerned in the $z' = 0$ plane without consideration of the influences of conduction and thermocapillary flow in the z'-direction.

The Boussinesq approximation is assumed to be valid for density variation in the melt, which means that density ρ satisfies the following relation:

$$\rho = \rho_m[1-\beta(T'-T_m)]. \quad (1)$$

The dependence of the surface tension on the temperature is assumed to be linear

$$\sigma(T') = \sigma_m - \gamma(T'-T_m) \quad (2)$$

where σ_m is the surface tension of the liquid at the melting temperature and constant γ is the rate of change of surface tension with temperature.

The results of the asymptotic solutions [9] and numerical computations [10] for thermocapillary flow in a rectangular cavity show that for a small capillary number the gas–liquid surface deformation is about $O(10^{-3})$ compared with the height of the cavity. The capillary number is defined by $Ca = \gamma\Delta T'/\sigma_m$ where $\Delta T'$ is the maximum temperature difference at the

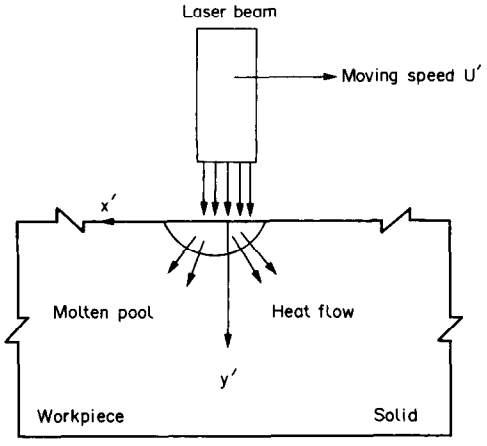

FIG. 1. Schematic diagram of the physical system.

gas–liquid interface. As mentioned by Srinivasan and Basu [5], the capillary number is much less than 1 for most molten metals during laser melting. Therefore, the free surface of the gas–liquid interface is assumed to be flat. In the present study we concentrate on the effect of the interaction of the thermocapillary convection with the moving heat source on the shape of the solid–liquid interface. In order to simplify the computation, the thermodynamic properties are assumed to be the same for both liquid and solid phases. In a real physical condition, the thermodynamic properties are different for solid and liquid phases. The results of Kou *et al.* [1] show that the temperature profiles and the shape of the melting pool do not alter using different values of thermodynamic properties in the solid and liquid phases and the influence on the melting depth depends on the order of difference. It is obvious that under this assumption, the physical characters are not changed significantly. The enthalpy H' is defined as follows:

$$H' = \rho C_p(T' - T_0) \quad \text{for } T' < T_m \tag{3a}$$

$$H' = \rho C_p(T_m - T_0) + \rho L' \quad \text{for } T' = T_m \tag{3b}$$

$$H' = \rho L' + \rho C_p(T' - T_0) \quad \text{for } T' \geqslant T_m. \tag{3c}$$

In this problem the convection flow pattern is driven dominantly by the shear stress induced by the surface tension gradient at the gas–liquid interface. By examining the shear-stress balance along the gas–liquid interface the characteristic velocity in the molten region can be obtained as follows:

$$U_c = \gamma q d/k\mu.$$

The following non-dimensional variables are introduced:

$$x = x'/d, \quad y = y'/d, \quad u = u'/U_c$$

$$v = v'/U_c, \quad U = U'/U_c, \quad L = L'/(qd/\rho\alpha)$$

$$p = p'/(\gamma q/k), \quad H = H'/(qd/\alpha)$$

$$T = (T' - T_0)/(qd/k). \tag{4}$$

The non-dimensional governing equations for the quasi-steady two-dimensional motion are

$$u_x + v_y = 0 \tag{5a}$$

$$Re(Uu_x + uu_x + vu_y) = -p_x + u_{xx} + u_{yy} \tag{5b}$$

$$Re(Uv_x + uv_x + vv_y) = -p_y + (v_{xx} + v_{yy}) + Gr\,T/Re \tag{5c}$$

$$Ma(UH_x + uH_x + vH_y) = H_{xx} + H_{yy} \tag{5d}$$

where $u = v = 0$ in the solid region. The Reynolds number, the Grashof number, and the Marangoni number are defined in the usual way by

$$Re = \gamma q d^2/(k\mu v) \tag{6a}$$

$$Gr = g\beta q d^4/(kv^2) \tag{6b}$$

$$Ma = Re\,Pr \tag{6c}$$

where the Prandtl number is given by $Pr = v/\alpha$. The Marangoni number Ma determines the relative importance of thermocapillary convection to thermal diffusion and the Reynolds number Re determines the relative importance of thermocapillary convection to viscous diffusion. The relationship between the enthalpy and temperature becomes

$$T = H \quad \text{for } H < H_s \tag{7a}$$

$$T = T_m \quad \text{for } H_s < H < H_l \tag{7b}$$

$$T = H - L \quad \text{for } H > H_l \tag{7c}$$

where

$$H_s = (T_m - T_0)k/qd, \quad H_l = H_s + L. \tag{7d}$$

The boundary conditions are

$$v = 0$$

$$u_y = H_x$$

$$H_y = \begin{cases} -1 & |x| < 1.0 \\ 0 & |x| > 1.0 \end{cases} \quad \text{at } y = 0 \tag{8a}$$

$$\left.\begin{aligned} u &= 0 \\ v &= 0 \\ H &= H_l \end{aligned}\right\} \quad \text{at } S(x, y) = 0 \tag{8b}$$

$$H \to 0 \quad \text{as } |x|, y \to \infty. \tag{8c}$$

In conditions (8b), $S(x, y) = 0$ is the interface between the solid and the liquid region.

In the present system, the effect of buoyancy driven flow can be neglected as compared to the surface tension driven flow. Eliminating the pressure from equations (5) we obtain

$$Re(U\xi_x + \psi_y\xi_x - \psi_x\xi_y) = \xi_{xx} + \xi_{yy} \tag{9a}$$

$$Ma(UH_x + \psi_y H_x - \psi_x H_y) = H_{xx} + H_{yy} \tag{9b}$$

$$\xi = -(\psi_{xx} + \psi_{yy}) \tag{9c}$$

where the stream function ψ is given by

$$u = \psi_y, \quad v = -\psi_x \tag{10}$$

and the vorticity is given by

$$\xi = v_x - u_y. \tag{11}$$

The boundary conditions are

$$\left.\begin{aligned} &\psi = 0 \\ &\xi_y = -H_x \\ &H_y = \begin{cases} -1 & |x| < 1.0 \\ 0 & |x| > 1.0 \end{cases} \end{aligned}\right\} \quad \text{at } y = 0 \tag{12a}$$

$$\left.\begin{aligned} &\psi = 0 \\ &\xi = -(\psi_{xx} + \psi_{yy}) \\ &H = H_1 \end{aligned}\right\} \quad \text{at } S(x, y) = 0 \tag{12b}$$

$$H \to 0 \qquad \text{as } |x|, y \to \infty. \tag{12c}$$

3. NUMERICAL PROCEDURE

During surface melting there is a small molten region on the surface of the workpiece, where the large temperature and velocity gradients exist. It is necessary to place more grid points in the molten region than in the solid region. Analytical coordinate transformations which are used to optimize the grid point placement and transform a non-uniform grid in the physical domain into an equally spaced grid in the computation domain are given by

$$\kappa = \kappa_t\{B + \sinh^{-1}[(2x/X)\sinh(aB)]/a - 0.5\} \tag{13a}$$

$$\eta = \eta_t(1 - e^{-by/Y})/(1 - e^{-b}) \tag{13b}$$

where

$$B = \frac{1}{2a}\ln\left[\frac{1 + (e^a - 1)/2}{1 + (e^{-a} - 1)/2}\right]; \tag{14}$$

X and Y are the lengths of the physical domain in the x- and y-directions, respectively; κ_t and η_t are the lengths of the computational domain in the κ- and η-directions, respectively; a and b are the stretching parameters which vary from zero (no stretching) to large values which produce the most refinement near the origin. A typical grid point distribution in the physical domain produced by equations (13) is shown in Fig. 2.

The governing equations (9) and boundary condition (12) are expressed in terms of transformation and then finite-difference equations are constructed using a second-order accurate expression. It is worth pointing out that the solid–liquid interface, $S(x, y) = 0$, is not known a priori, and is a part of the solution. In the present paper we adopt the H_1 value to locate the position of the solid–liquid interface. If H is greater than H_1, then ξ, ψ and H are to be solved by the governing equation (9). If H is less than H_1, then only the conduction equation is solved. On account of the solid–liquid interface being a curved delineation, the momentum equation adjacent to the interface must be carefully handled. At this step we use a finite-difference representation of the second-order derivative at a node near a curved boundary [11].

The solution of the difference equation starts from

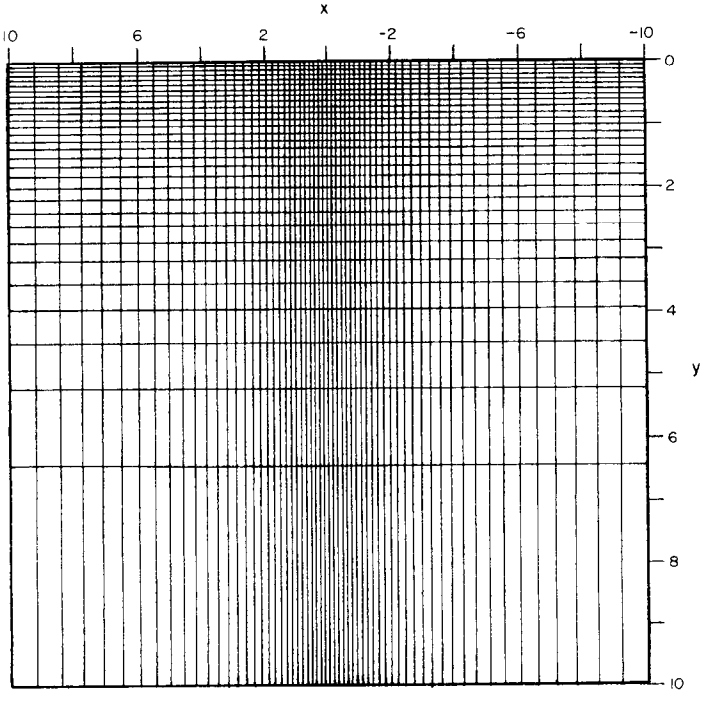

FIG. 2. The distribution of the (61 × 31) grid points in the physical plane with stretching parameters $a = 5$, $b = 5$.

an initial shape of the solid–liquid interface determined by solving the pure conduction equation. The initial guesses for ψ and ξ in the liquid region are selected. The difference equation for ξ is solved at iteration $m+1$ using ψ and H from iteration m to form the coefficients in the non-linear terms and boundary conditions. The derivatives in the x-direction are treated implicitly while derivatives in the y-direction are treated explicitly. After the new ξ is obtained, the difference equation ψ and H can be solved iteratively using line successive over-relaxation (LSOR) with an approximated optimized relation factor for a given mesh. The new solutions of stream function and enthalpy are then used to correct the solid–liquid interface and the initial guesses of ψ and H. The procedure can be repeated until the difference between two subsequent computations is within a specified tolerance. For the present study, the relative error criterion is chosen as $|(\phi^{new}-\phi^{old})/\phi^{max}| < \varepsilon$, where ϕ is any physical variable. The value of ε is chosen as 0.0001 for the solution of ψ and H and 0.0025 for the solution of ξ.

4. RESULTS AND DISCUSSION

The computation domain must be chosen large enough to fit the proper assumption of semi-infinite space. In the present study, the dimensionless width and depth, are selected as 20 and 10, respectively. The (81×41) grids are used in the computational domain. We select grid control parameters $a = 10$ and $b = 10$ to show that there are (51×21) grids in the molten region. The typical distribution of dimensionless surface enthalpy is shown in Fig. 3. It attains a maximum value near the centre and approaches zero as $|x| > 3$. The temperature gradient becomes the greatest near the edge of the laser beam ($|x| = 1$). Kou *et al.* [1] considered the present problem without consideration of the influence of thermocapillary convection. In order to check our results, we have repeated the calculation with the same conditions. The present results agree with those of Kou *et al.* [1]. The effect of the latent heat of fusion on the melting zone is of interest. Figure 4 shows the interface shapes of $Ma = 100$,

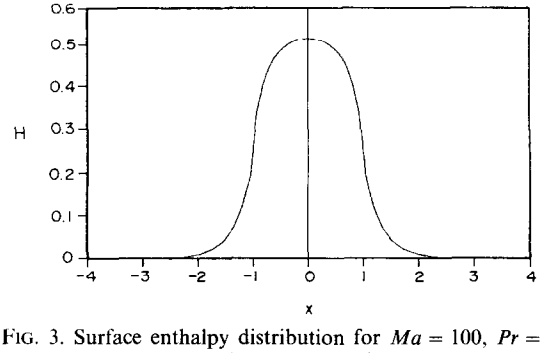

FIG. 3. Surface enthalpy distribution for $Ma = 100$, $Pr = 0.01$, $U = 0.00001$, $H_s = 0.2$, and $H_l = 0.25$.

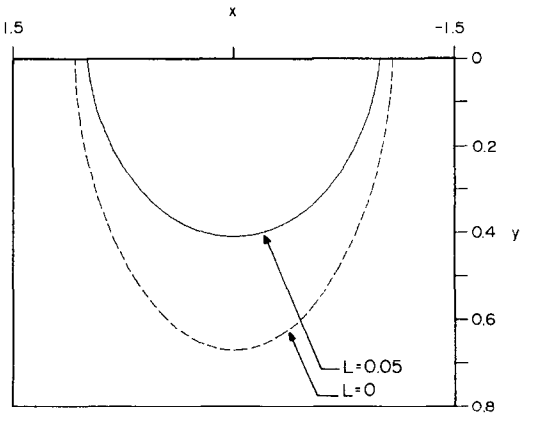

FIG. 4. Interface shapes for $Ma = 100$, $Pr = 0.01$, $U = 0.00001$, and $H_s = 0.2$ with $L = 0$ and 0.05.

$Pr = 0.01$, $H_s = 0.2$ with $L = 0$ and 0.05. The case of $L = 0$ corresponds to the case when the latent heat effect is excluded. The melting region without the consideration of latent heat of fusion is larger than that with the latent heat effect. Under the same Re the

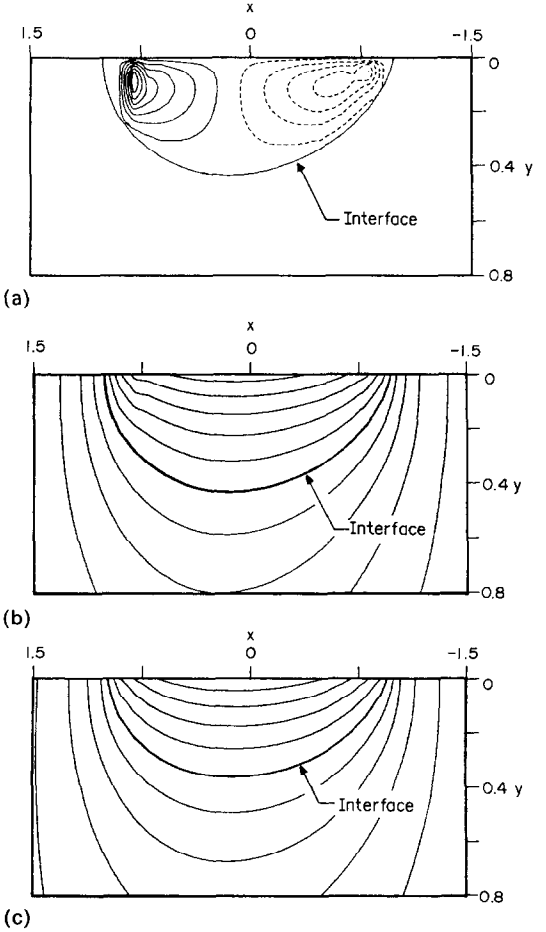

FIG. 5. Contours for (a) streamlines, (b) isothermal lines for convection and (c) isothermal lines for conduction, with $Ma = 1000$, $Pr = 0.1$, $U = 0.0008$, $H_s = 0.2$, $L = 0.05$, and $H_l = 0.25$.

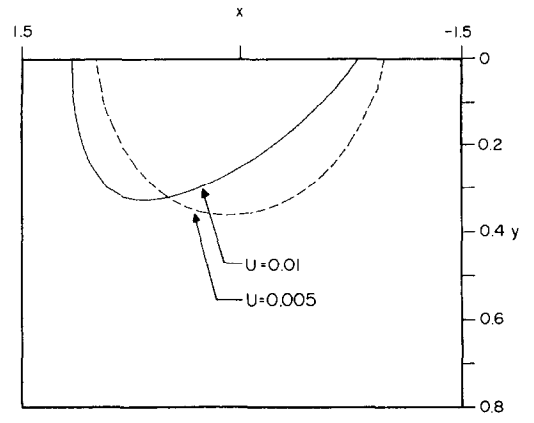

FIG. 6. Interface position for $Ma = 500$, $Pr = 0.1$, and $H_1 = 0.25$ with $U = 0.01$ and 0.005.

magnitudes of H_s and L for pure aluminium and Al–Mg–Si alloy (6061 aluminium) are 0.4826, 0.2814 and 0.2255, 0.133, respectively. It is obvious that the latent heat of fusion for the metals has a profound effect on determining the melting shape.

Figures 5(a) and (b) demonstrate that the isothermal lines and streamlines are no longer symmetrical about the central line owing to the influence of the external moving heat source. In general, the surface tension temperature coefficient γ is positive for the liquids. Thus the surface tension at the edge of the molten region is maximum while the surface tension beneath the centre of the moving heat flux is minimum. Therefore, along the liquid–gas free surface, there is a surface-tension gradient which produces a radial outward motion from the centre of highest temperature to the edge of the molten region. The thermocapillary force driving the fluid particles to the direction of increasing surface tension is balanced by the viscous shear stress at the liquid–gas interface fluid, and it results in inducing the bulk motion of the fluid. In Fig. 5(a) there are two vortices on the counter sides of the pool and the streamlines are closer and the velocities are faster near the liquid–gas interface. The velocity is higher near the edge of the melting pool because the maximum temperature gradient occurs near $|x| = 1$ (Fig. 3). Unlike the previous results [5, 6], the two vortices have different sizes and are asymmetric along the centre of the laser beam ($x = 0$). The vortex near the trailing end of the scanning velocity is stronger than that near the leading edge. The isothermal lines shown in Fig. 5(c) are obtained by conduction only. In comparing Figs. 5(b) and (c), we can see that due to the presence of the bulk flow, the depth of the melting pool is increased and the isothermal lines are modified significantly near the edge of the melting pool. The heat transfer by convection is enhanced in the y-direction and the temperature profile is twisted in the x-direction. The scanning velocity U determines the absorbed energy per unit area of the workpiece. It is obvious that the faster the velocity scans over the workpiece, the less energy will be absorbed. Figure 6 demonstrates the influence of the moving velocity U on the shape of the melting region. The increasing value of U will shift the solid–liquid interface to the trailing end of the moving external heat source and increase the distortion of the molten pool. When the values of U increase the maximum depth of the melting pool decreases and the

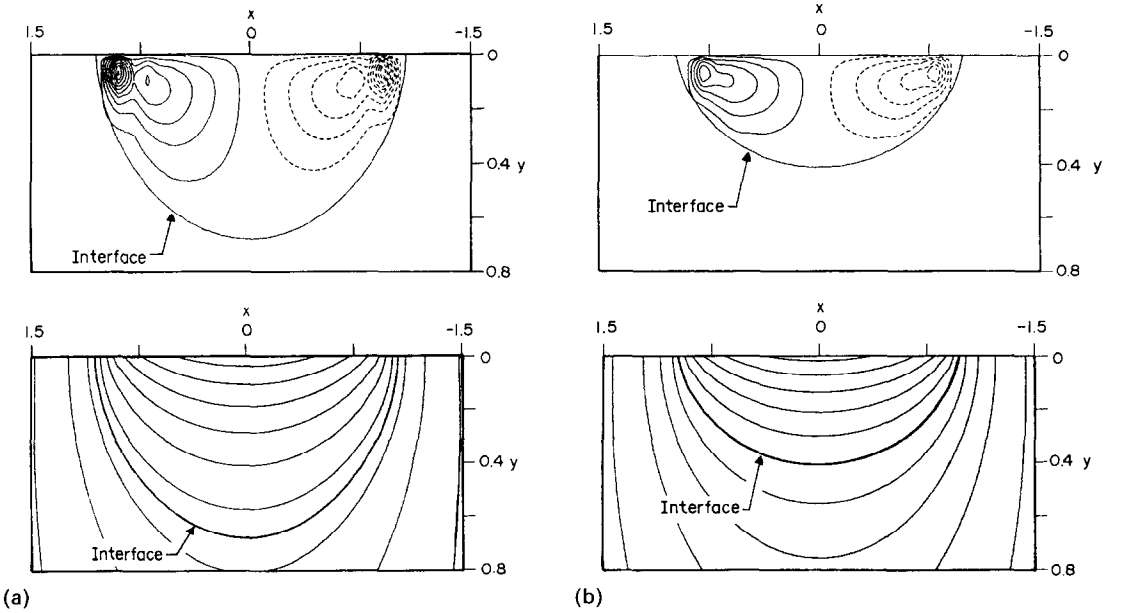

FIG. 7. Contours for streamlines and isothermal lines for different Marangoni number: (a) $Ma = 120$, $Pr = 0.01$, $H_1 = 0.25$, and $U = 0.00001$; (b) $Ma = 100$, $Pr = 0.01$, $H_1 = 0.25$, and $U = 0.00001$.

pool region gets smaller. The present results display that the pool shape is changed significantly by the external moving heat source.

Figure 7 shows the effect of Marangoni number Ma (or Re) with Pr fixed. When Ma is large, the fluid flow is so vigorous that the counter-rotating vortex carries higher energy particles down to the melt and then leads to deeper penetration in the pool. The present results are consistent with those of Chan *et al.* [7] and Basu and Srinivasan [6] in that the melting depth increases with increasing values of Ma. For $Ma = 120$, the formation of twin secondary cells appears at both corners.

It is interesting to note that the Prandtl number Pr is defined as the ratio of kinematic viscosity and heat diffusivity. As Pr increases, the material is heated up slowly. Thereby the thermal diffusion becomes more difficult. It can be expected that the melting depth will decrease with higher Pr. The influence of Pr on the shape of the pool is illustrated in Fig. 8. This result is consistent with that of Chan *et al.* [7] in that the ratio of width to depth of the melting pool increases with increasing Pr. Furthermore, it is obvious that the effect of scanning velocity is more significant for higher Pr. The present results demonstrate that for higher Pr the interface position is shifted increasingly toward the trailing edge owing to the momentum effect generated by the scanning velocity of the heat source. The isothermal lines and streamlines in the molten region for different Marangoni number Ma (or Pr) with Re fixed are shown in Figs. 9 and 10. With the consideration of the effect of thermocapillary convection, the melting depth is increased significantly and the melting width is enlarged slightly for $Ma = 50$, while the melting depth is decreased and the melting width is increased for $Ma = 10\,000$. When $Ma = 10\,000$ the solid–liquid interfaces for both conduction and convection obviously shift to the opposite direction of scanning velocity. In comparison with the case of $Ma = 50$, the streamline and isotherm patterns

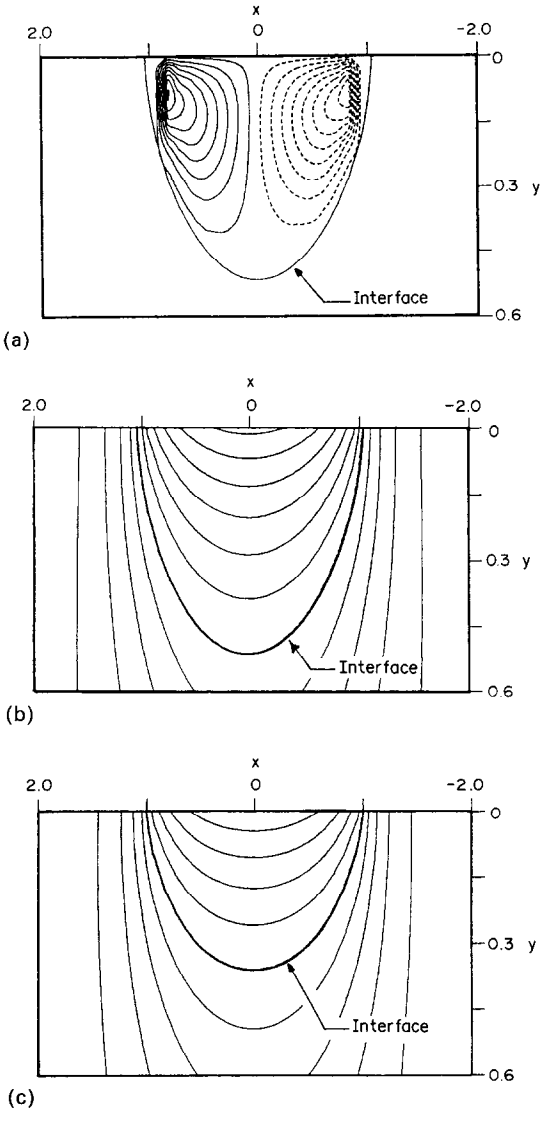

FIG. 9. Contours for (a) streamlines, (b) isothermal lines for convection and (c) isothermal lines for conduction, with $Ma = 50$, $Pr = 0.01$, $U = 0.0005$, $H_s = 0.2$, $L = 0.05$, and $H_l = 0.25$.

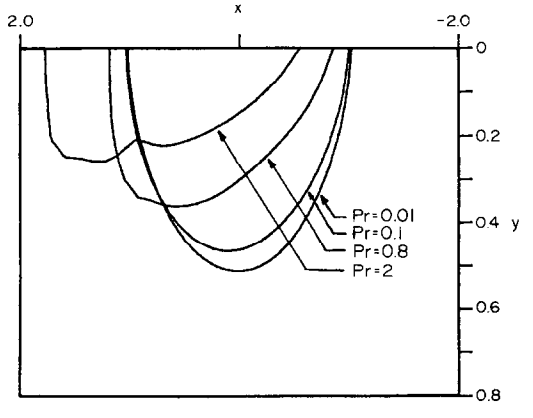

FIG. 8. Interface position for $Re = 5000$, $U = 0.0005$, and $H_l = 0.25$ with $Pr = 0.01$, 0.1, 0.8, and 2.0.

are modified dramatically. Near the trailing edge of the melting pool there exists a vortex of twin secondary cells which is stronger than that near the leading edge.

5. SUMMARY

The finite-difference method with grid-stretching transformation has been employed to study the heat- and fluid-flow phenomena in a melting pool generated by high energy power laser impinging on a semi-infinite workpiece. The results presented in this paper reveal many important aspects of surface tension convection (also called thermocapillary con-

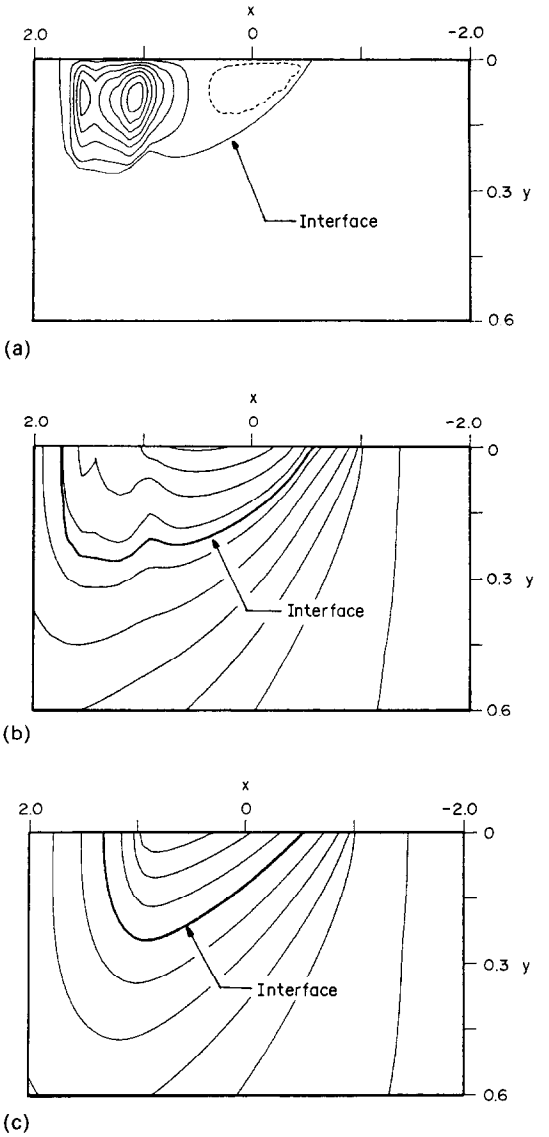

FIG. 10. Contours for (a) streamlines, (b) isothermal lines for convection and (c) isothermal lines for conduction, with $Ma = 10000$, $Pr = 2.0$, $U = 0.0005$, $H_s = 0.2$, $L = 0.05$, and $H_l = 0.25$.

vection) in the melt. The principal findings of the work may be summarized as follows:

(1) Contrary to the previous results of Chan *et al.* [7], the present results show that the size of the melting pool is reduced significantly when the effect of latent heat of fusion is included.

(2) We find and validate that the scanning velocity has a pronounced influence on the flow pattern and shape of the melting pool. For faster scanning velocity, the melting depth decreases and the melting shape distorts more drastically.

(3) The depth of the melting pool increases with an increase in the Marangoni number at fixed Prandtl number. This results from the increasing strength of the thermocapillary convection.

(4) The melting depth decreases with an increase in the Prandtl number. The flow fields, the temperature fields, and the melting shape are strongly influenced by the interaction of thermocapillary convection with the scanning velocity of the heat source if the fluid has high Prandtl number.

Acknowledgements—The authors gratefully acknowledge the support of the National Science Council of R.O.C. on this work through grant No. NSC77-0401-E008-07.

REFERENCES

1. S. Kou, S. C. Hsu and R. Mehrabian, Rapid melting and solidification of a surface due to a moving heat flux, *Metall. Trans.* **12b**, 33–45 (1981).
2. Y. Arata, N. Abe and T. Oda, Beam hole behavior during laser beam welding, *Proc. ICALEO '83*, pp. 59–66 (1983).
3. C. W. Draper and J. M. Poate, Laser surface alloying, *Int. Metal Rev.* **30**(2), 85–108 (1985).
4. T. R. Anthony and H. E. Cline, Surface rippling induced by surface tension gradients during laser surface melting and alloying, *J. Appl. Phys.* **48**, 3888–3894 (1977).
5. J. Srinivasan and B. Basu, A numerical study of thermocapillary flow in a rectangular cavity during laser melting, *Int. J. Heat Mass Transfer* **29**, 563–571 (1986).
6. B. Basu and J. Srinivasan, Numerical study of steady-state laser melting problem, *Int. J. Heat Mass Transfer* **31**, 2331–2338 (1988).
7. C. Chan, J. Mazumder and M. M. Chen, A two dimensional transient model for convection in laser melted pool, *Metall. Trans.* **15a**, 2175 2184 (1984).
8. G. M. Oreper and J. Szekely, Heat- and fluid-flow phenomena in weld pools, *J. Fluid Mech.* **147**, 53–79 (1984).
9. A. K. Sen and S. H. Davies, Steady thermocapillary convection in two dimensional slots, *J. Fluid Mech.* **121**, 163–186 (1982).
10. J. C. Chen, J. C. Sheu and S. S. Jwu, Numerical computation of thermocapillary convection in a rectangular cavity, *Numer. Heat Transfer A* **17**, 287–308 (1990).
11. M. Necati Ozisik, *Heat Conduction*, p. 513. Wiley, New York (1980).

ECOULEMENT THERMOCAPILLAIRE DE SURFACE EN FUSION DU A UN FLUX DE CHALEUR MOBILE

Résumé—L'écoulement et le transfert thermique convectif qui se produisent pendant la fusion laser sont examinés à la surface à l'aide d'une série de calculs numériques. Les équations du mouvement et de l'énergie sont résolues par une méthode aux différences finies avec une transformation de déformation de grille qui place plus de mailles dans la région de fusion. On considère les effets de la convection thermocapillaire dans le bain et la vitesse de déplacement de la source externe de chaleur sur la forme de l'interface solide–liquide. Les résultats montrent que la chaleur latente de fusion et différents parametres sans dimension associés au flux de chaleur mobile ont des effets importants sur la fusion.

THERMOKAPILLARE STRÖMUNGEN BEIM OBERFLÄCHENSCHMELZEN IN ANWESENHEIT EINER BEWEGLICHEN WÄRMEQUELLE

Zusammenfassung—Mit Hilfe einer Reihe von numerischen Berechnungen wird die Konvektionsströmung und der Wärmeübergang beim Anschmelzen einer Oberfläche mittels Laser untersucht. Die Gleichungen für Impulstransport und Energie werden mit Hilfe eines Finite-Differenzen-Verfahrens unter Verwendung einer Transformation zur Gitterstreckung gelöst, wodurch im geschmolzenen Gebiet mehr Gitterpunkte untergebracht werden können. Der Einfluß der thermokapillaren Konvektionsströmung in der Schmelze und der Bewegungsgeschwindigkeit der äußeren Wärmequelle auf die Form der Fest/Flüssig-Grenzfläche wird untersucht. Es zeigt sich, daß die Schmelzwärme und unterschiedliche dimensionslose Parameter, welche die bewegliche äußere Wärmequelle beschreiben, einen starken Einfluß auf die Bestimmung der Schmelzform ausüben.

ТЕРМОКАПИЛЛЯРНЫЕ ТЕЧЕНИЯ ПРИ ПЛАВЛЕНИИ ТЕЛА, ВЫЗВАННОМ ДВИЖУЩИМСЯ ТЕПЛОВЫМ ИСТОЧНИКОМ

Аннотация—При помощи численных расчетов исследуются конвективный теплоперенос и течение жидкости в процессе лазерой плавки. Уравнения количества движения и уравнение энергии решаются конечно-разностным методом с преобразованием, деформирующим сетку, при котором увеличивается количество точек сетки, попадающих в область расплава. Исследуется влияние термокапиллярной конвекции в расплаве и скорости движения внешнего источника тепла на форму границы раздела твердое тело–жидкость. Полученные результаты показывают, что форма расплава в большой степени зависит от теплоты плавления и различных безразмерных параметров, характеризующих движущийся постоянный тепловой источник.